Sub-Ambient Radiative Cooling Realized Using CaCO3 Microparticle-Based Single Layer Without Metal Reflector for Entire Day

Hangyu Lim
Korea University
Dongwoo Chae
Korea University
Soomin Son
Korea University
Sucheol Ju
Korea University
Jisung Ha
Korea University
Heon Lee (heonlee@korea.ac.kr)
Korea University

Research Article

Keywords: radiative cooling, micro-particle, broadband mid-IR emitter, atmospheric transparency window, passive cooling

Posted Date: May 24th, 2021

DOI: https://doi.org/10.21203/rs.3.rs-523745/v1

Sub-ambient radiative cooling realized using $CaCO_3$ microparticle-based single layer without metal reflector for entire day

*Hangyu Lim, Dongwoo Chae, Soomin Son, Sucheol Ju, Jisung Ha and Heon Lee**

Department of Material Science and Engineering, Korea University, Anam-ro 145, Sungbuk-Gu, Seoul 136-701, Republic of Korea

E-mail: nanoimprint@naver.com

Author information

Hangyu Lim: limhangyu96@gmail.com

Dongwoo Chae: dwc0808@korea.ac.kr

Soomin Son: wavry3330@naver.com

Sucheol Ju: vxz091@korea.ac.kr

Jisung Ha: hajisung3478@korea.ac.kr

*Heon Lee**: heonlee@korea.ac.kr

ABSTRACT

Conventional cooling systems, that is, air conditioners, should be replaced because they consume a substantial amount of energy and cause environmental pollution. In this context, radiative cooling systems, which perform cooling without consuming any energy or causing environmental pollution, are emerging as an alternative. However, most of the radiative coolers explored thus far include metals, such as silver, that are used as solar reflectors, thereby entailing problems in terms of practicality, mass production, cost, and light pollution. Herein, we propose calcium carbonate ($CaCO_3$) micro-particle-based radiative cooling, which utilizes the high-energy band gap of $CaCO_3$ for high-performance radiative cooling. As the cooler has only a single layer of a $CaCO_3$ composite without any metal reflector, it is mass-producible, cheap, and does not cause light pollution. To demonstrate the cooling performance of $CaCO_3$, optical properties and temperature changes are measured and compared with those of commercial white paint. As a result, it is demonstrated that the $CaCO_3$-based radiative cooler has cooling power 93.1 W/m^2 in calculation and can be cooled 6.52 ℃ and 3.38 ℃ under ambient temperature in daytime and nighttime respectively. Thus, it can perform as radiative cooler in entire day.

KEYWORDS: radiative cooling, micro-particle, broadband mid-IR emitter, atmospheric transparency window, passive cooling

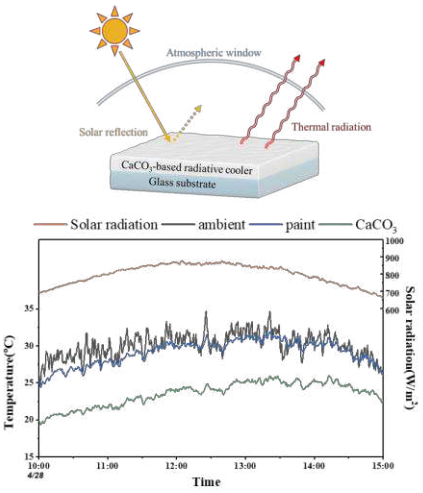

1. Introduction

Cooling systems are a crucial necessity in modern industrial and residential complexes. Presently, most cooling systems incorporate air conditioners. However, air conditioners consume large amounts of energy and are a major cause of environmental pollution, such as the emission of chlorofluorocarbons, which lead to ozone depletion[1]. Moreover, the most of energy used to drive the air conditioner obtained by consuming fossil fuels which emit greenhouse gases that cause global warming. Therefore, a new type of cooling system is required. In this scenario, radiative cooling is the key to an alternative cooling system. Notably, radiative cooling entails thermodynamic cooling without any energy consumption. Consequently, it does not burden the environment[2,3]. The principle of passive radiative cooling is that the system radiates its energy in the form of infrared rays with a wavelength of 8–13 μm (referred to as the atmospheric window) and reflects sunlight which means the system is not heated by solar radiated energy[4,5]. Unlike a conventional cooling system that transfers heat from the inside to the outside, a radiative cooler emits energy directly into space, at a temperature of 3 K, without entailing any chemical reactions or harmful effects to living beings. Because it radiates energy directly into space, it does not cause global warming, in contrast with air conditioners.

Substantial research on sub-ambient radiative cooling has been actively conducted over the past few years, including investigating multilayer thin films[2,5,6,7], polymer-based radiative coolers[8,9,10], and photonic material structures[6,11,12,13] and their various applications [12,14,15,16,17]. However, most radiative coolers include silver reflectors to reflect sunlight, which causes certain problems. Silver is expensive and easily oxidized, and high vacuum equipment is required to deposit it. Oxidized silver absorbs solar energy, which has a negative effect on radiative cooling. Using high vacuum deposition, silver would be required to be deposited on a flat surface, which would impose a constraint on the choice of the substrate; in addition, the process cost would also be high. Furthermore, silver is a specular reflector that causes light pollution[18]. Smooth surface reflectors, such as mirrors, reflect light parallelly, which can cause dizziness or safety hazards for pedestrians and drivers. It can also damage the retina or iris, causing vision loss in certain cases. Owing to these reasons, researchers have recently published radiative coolers without a metal reflector. In order to reflect sunlight without a metal layer, white ceramic powders such as SiO_2, Al_2O_3 are mixed with the polymer matrix[19,20,21], a porous polymer[4] or a polymer composite[22] is prepared to induce scattering to increase the reflectivity. These can radiate and be cooled without metal reflector, but because they are composed of a polymer matrix, they are susceptible to scratches due to their low hardness. Therefore, in this study, the performance of a ceramic powder-based radiative cooling device using $CaCO_3$ microparticles(MPs) will be discussed.

$CaCO_3$ is inexpensive and has excellent thermal and mechanical stability. Consequently, it is used as a filler in several composite materials. Further, it is mainly used in plastics[23,24,25,26], dyes[27,28], and rubber.[29] It is also widely used in agricultural chemicals[30,31], medicine[32,33], food[34], and construction materials[35,36]. Moreover, due to its large band gap of 5 eV, it does not absorb

most of solar irradiance. We demonstrate the radiative cooling performance of $CaCO_3$ by comparing it to that of a commercial white paint.

2. Principle of radiative cooling

The equation for radiative cooling is derived using the law of conservation of energy as follows[23,37]:

$$P_{\text{net}}(T) = P_{\text{rad}}(T) - P_{\text{atm}}(T_{\text{atm}}) - P_{\text{sun}} - P_{\text{non-rad}} \quad (1)$$

where

$$P_{\text{rad}}(\text{T}) = \int_0^{2\pi} \int_0^{\frac{\pi}{2}} \int_0^{\infty} I_{\text{BB}}(T, \lambda)\, \varepsilon(\lambda, \theta) \cos\theta \sin\theta \, d\lambda \, d\theta \, d\varphi \quad (2)$$

represents the hemispherical radiation power emitted from the radiative cooler.

$$P_{\text{sun}} = \int_0^{\infty} I_{AM1.5}(\lambda) \varepsilon(\lambda, \theta) \, d\lambda \quad (3)$$

is the solar irradiance power absorbed by the radiative cooler.

$$P_{\text{atm}}(T_{\text{atm}}) = \int_0^{2\pi} \int_0^{\frac{\pi}{2}} \int_0^{\infty} I_{\text{BB}}(T_{\text{atm}}, \lambda) \varepsilon(\lambda, \theta) \varepsilon_{\text{atm}}(\lambda, \theta) \cos\theta \sin\theta \, d\lambda \, d\theta \, d\varphi \quad (4)$$

is the power of the incident atmospheric radiation. According to Kirchhoff's law of thermal radiation, for these equations, absorption and radiation are the same owing to thermodynamic equilibrium.

$$P_{\text{non-rad}} = h_{\text{c}}(T_{\text{atm}} - T) \quad (5)$$

denotes the power lost by the radiative cooler because of convection and conduction.

Here, I_{BB} represents the blackbody radiation intensity and is expressed using the formula $I_{BB} = (2hc^2/\lambda^5) \times (e^{hc/\lambda k_B T} - 1)^{-1}$, and $\varepsilon_{\text{atm}}(\lambda, \theta) = 1 - [t(\lambda)]^{1/\cos\theta}$ represents the

angular atmospheric emissivity, where $t(\lambda)$ denotes the atmospheric transmittance in the zenith direction. The constants h_c, h, c, k_B represent the heat transfer coefficient, the Planck constant, speed of light, and Boltzmann constant, respectively. The cooling temperature is defined as $\Delta T_{\mathrm{cool}} = T - T_{\mathrm{atm}}$, which is calculated by extracting the cooling temperature under the condition $P_{\mathrm{net}}(T) = 0$. As previously reported, T_{atm} is replaced by T_{amb}[38,39]. All the calculation processes of the net cooling power and cooling temperature were performed using MATLAB software based on absorptivity and emissivity values, with a wavelength spacing of 0.01 μm.

3. Experimental

3.1. Source materials

dipentaerythritol penta-/hexa-acrylate, 1-hydroxycyclohexyl phenyl ketone 99% (Irgacure 184, photoinitiator), calcium carbonate powder (20–30 μm in diameter), and 1-methyl-2-pyrrolidinone (NMP) were purchased from Sigma Aldrich. For comparison, commercial white paint was acquired from Okong Company in spray form.

3.2. Sample preparation

$CaCO_3$ MP (5 g) was mixed in NMP (intrinsic solvent) (5 g) and stirred at 200 rpm with a magnetic stirring bar for 30 min so that it would not agglomerate with each particle. After the powders were dispersed, the DPHA monomer (0.25 g) and UV initiator (Irgacure 184) (0.025 g) were added to the solution and stirred at 200 rpm for 2 h. The glass substrate was treated with UV-ozone, the prepared solution was dropped on it, and the glass with the solution was

heated on a 100 °C hot plate for 2 h to evaporate the NMP solution. After the solvent had dried completely, it was exposed to a UV lamp for 30 min to polymerize the DPHA.

To prepare paint-coated glass, the glass was spray painted to make it approximately 200 μm thick.

3.3. Sample Characterization

An X-ray powder diffraction (XRD) scan (SmartLab, Rigaku, Japan) was performed using a diffractometer and a Cu target (wavelength: 1.5412 A) as the X-ray source at 9 kW. The surface of the radiative cooler was observed at 15 keV using FESEM (Regulus8100, Hitachi, Japan). Optical properties within a wavelength range of 3–2.5 μm were measured using a UV-Vis-NIR spectrophotometer (Solidspec-3700, Shimadzu, Japan) in the integral sphere using Spectralon diffuse reflectance standards (SRS-99-010, Labsphere, USA) as a baseline reflector. The optical properties of the IR spectra (wavelength range of 3–15 μm) were measured through Fourier transform infrared spectroscopy (FT-IR; Nicolet IS-50, Thermo Scientific, USA) and an integral sphere (Mid-IR IntegratIRTM, PIKE technologies, USA) using an Au reflector. The absorbance A was determined using the equation A=1-R-T after measuring the reflectance R and transmittance T using the equipment described.

4. Results and discussion

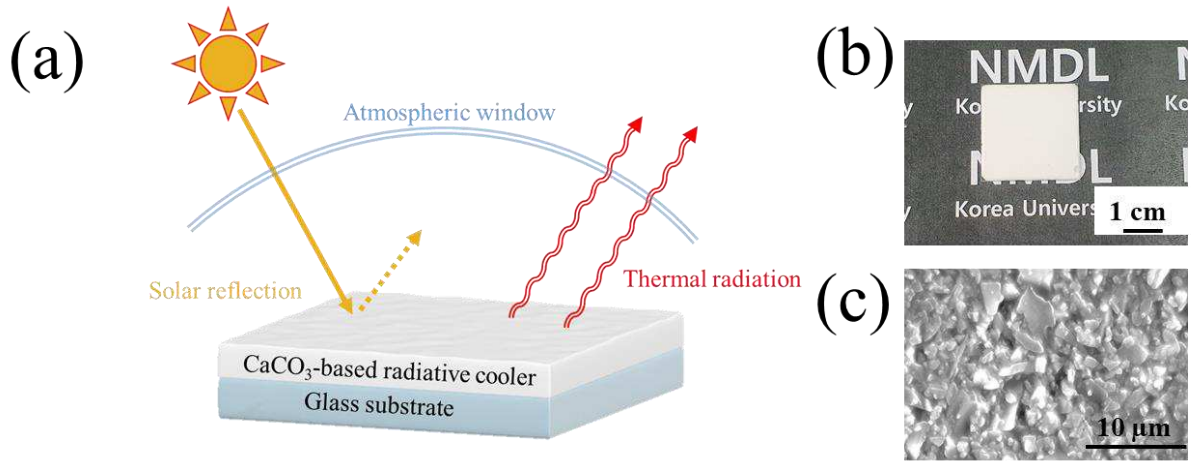

Figure 1. (a) Schematic of radiative cooling principle and radiative cooler structure. (b) Photo image and (c) SEM top view of radiative cooler, $CaCO_3$-coated glass.

Figure 1(a) shows the operating principle of radiative cooling and structure of $CaCO_3$-based radiative cooler. By reflecting sunlight, it avoids being heating and sends heat energy to the outside by radiating infrared rays in the wavelength range corresponding to the atmospheric window, cooling to a lower temperature than the ambient temperature. As depicted in Figure 1(b), the $CaCO_3$ layer is coated on glass placed over a black background, and the letters in the background are not visible, indicating that the transmittance is sufficiently low in the visual check. Figure 1(c) displays the surface of the $CaCO_3$ layer analyzed through field emission scanning electron microscopy (FESEM). Figure S2 depicts the absorption and transmittance of $CaCO_3$ with the dipentaerythritol penta-/hexa-acrylate (DPHA) binder with respect to the thickness. With an increase in the thickness, the transmittance tends to decrease. However, the absorption did not increase until the thickness reached 350 μm. Further, at 500 μm, the absorption started increasing, and approximately 8% of the solar incident power was absorbed. The emissivity within the atmospheric window region does not differ significantly based on the thickness. The ratio of absorbed solar incident power, average emissivity in the atmospheric

window region, and calculated net cooling power at 300 K in accordance with the thickness are listed in Table S1. The cooling power is the highest at a thickness of 130 μm; however, because the transmittance in the solar radiation region is greater than 5%, the thickness of 350 μm, at which the transmittance is low and the absorption does not increase significantly, is considered to be the most suitable and is adopted as the thickness used in this experiment.

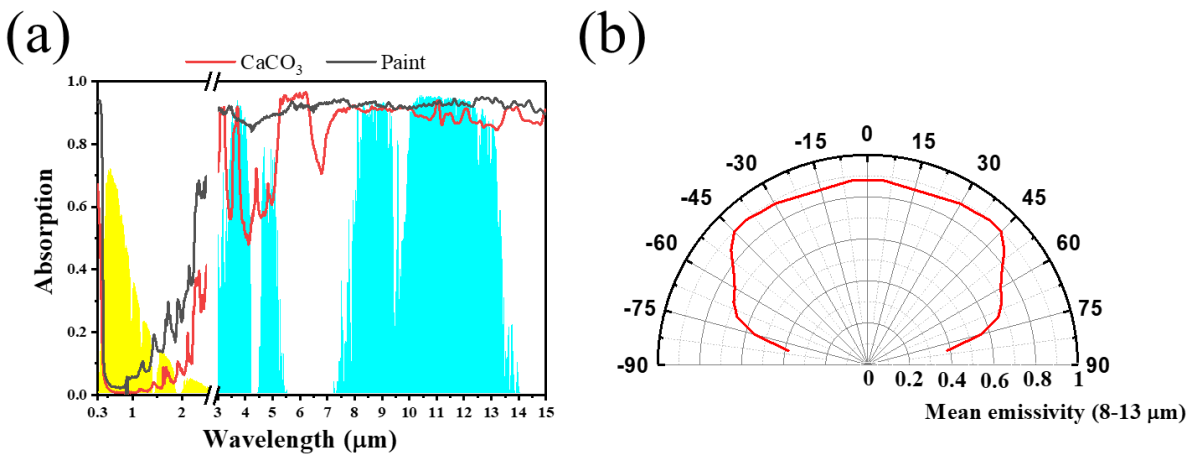

Figure 2. (a) Spectral absorptivity and emissivity of $CaCO_3$- and commercial white-paint-coated glass. (b) Average emissivity of $CaCO_3$-coated glass in the atmospheric window (8–13 μm) with respect to angle θ.

Figure 2(a) presents the absorption properties of $CaCO_3$ and white-paint-coated glass. In the atmospheric window region, $CaCO_3$ and the paint have emissivities of 89.6% and 92.7%, respectively. The paint has a slightly better emissivity property. However, in the solar radiation region, $CaCO_3$ has better absorption properties than the paint. $CaCO_3$ absorbs 4.1% of the solar incident power, whereas the paint absorbs 11.1%. This difference in solar absorbption affects the cooling performance. Using these optical properties, at 300 K, the net cooling power was calculated as 93.1 W/m^2 for $CaCO_3$ and 38.6 W/m^2 for paint. The calculation shows that $CaCO_3$ demonstrates 2.4 times higher cooling performance than the paint. The ratio of absorbed solar incident power, average emissivity in the atmospheric window region, and net cooling power are presented in Table 1. Figure 2(b) depicts the average emissivity in the atmospheric window

167 region in accordance with the incident light angle. The decrease in emissivity starts at
168 approximately 50°, and the emissivity remains greater than 70% until the angle of 70° is
169 reached.

170 **Table 1**. Average absorption (0.3-2.5 μm), emissivity (8-13 μm) and net cooling power at 300 K

Sample	Solar power absorption ratio (0.3-2.5 μm)	Average emissivity (8-13 μm)	Net cooling power at 300 K (W/m^2)
$CaCO_3$	0.041	0.896	93.1
paint	0.111	0.927	38.6

171

172

173

174

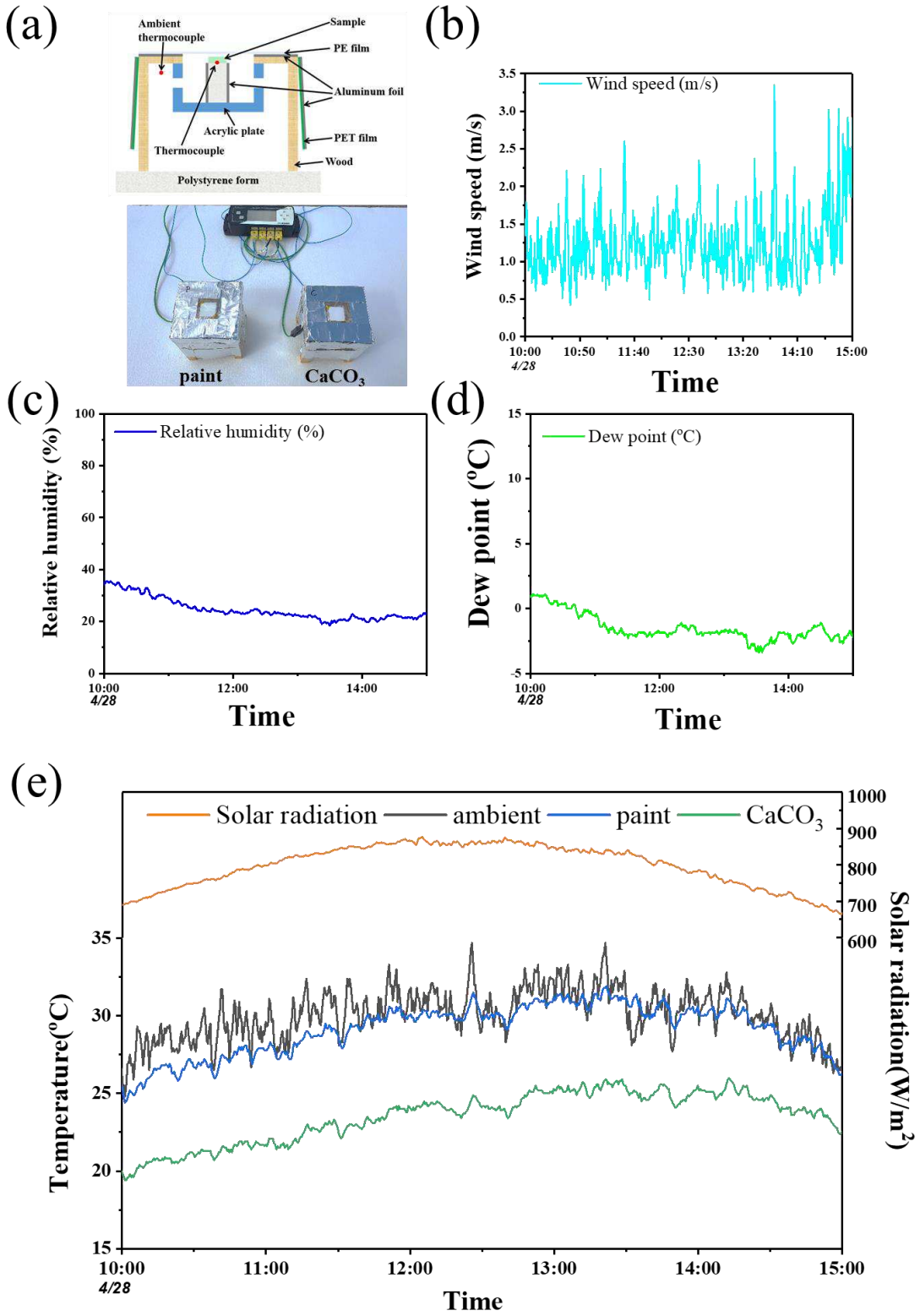

175

176 **Figure. 3**. (a) Schematic diagram and photo image of outdoor measurement system for radiative cooling.
177 Environmental conditions (b) wind speed, (c) Relative humidity, (d) dew point. (e) Radiative cooling performance
178 of $CaCO_3$ and white paint in terms of temperature in daytime.

To measure the variation in the temperature of the surroundings over time, a measurement chamber was prepared. A schematic of the chamber is presented in Figure 3(a). Acrylic plates are attached to a frame made of wood, except for the top side of the frame. To prevent conduction between the chamber frame and radiative cooler, a polystyrene pillar was attached to the center of the acrylic plate, and a radiative cooler sample with K-type adhesive thermocouples (ST-50, RKC INSTRUMENT INC., Japan) attached to the floor was placed on the pillar. Several holes were drilled into the sides of the acrylic plates to allow the air to reach an ambient temperature similar to the outside temperature; further, to reduce the influence of wind, Polyethlene Terephthalate (PET) films were attached to the side of the frame. The top side of the chamber was covered with low-density polyethylene (LDPE) to maximize radiative cooling effect by preventing the influence of the wind, but light of almost all wavelengths could be transmitted through the top side[4041]. Finally, all the sides of the chamber were covered with aluminum tape to reflect the light and prevent the chamber from being heated by the incident solar radiation. A copper wire thermocouple was attached to the inside of the PET film, such that the tip of the wire did not contact anything, to measure the ambient temperature. Although the LDPE film has excellent transmittance, it does not have perfect transmittance, as depicted in Figure S3(d), which causes a greenhouse effect that increases the inner temperature. Because of the greenhouse effect, holes were drilled into the acryl plates to maintain a temperature similar to that of the surroundings. The measurements were conducted on the roof of a new engineering hall at Korea University, Seoul, South Korea. The temperature of the samples and the ambient temperature were recorded every 30 s using a data logger (OM-CP-OCTTEMP-A, OMEGA Engineering, USA). The solar irradiance, wind speed, relative humidity, and dew point were also recorded every 30 s through a weather station (HD52.3D, DeltaOHM, Italy).

Figure 3(b), (c), and (d) depict the external daytime environmental conditions of wind speed, relative humidity, and dew point data, respectively, over time. The temperature variations in the $CaCO_3$- and paint-coated glasses, ambient temperature, and solar irradiation power from 10:00 to 15:00 are depicted in Figure 3(e). The figures indicate that the weather is clear, not cloudy, and that the fluctuation in solar irradiation is not large. The temperature of the paint-coated glass was lower by an average of 0.93 ℃ when compared with the ambient temperature from 10:00 to 15:00. This cooling is not significantly meaningful, as the difference in temperature was less than 1 ℃. On the other hand, the temperature of the $CaCO_3$-coated glass was lower than the ambient temperature by an average of 6.52 ℃ during the same time. Based on optical properties, it is clear that paint can emit more energy than $CaCO_3$ through the atmospheric window. However, it absorbs a substantial amount of solar radiated power, which negatively affects the radiative cooling performance. On the other hand, although $CaCO_3$-coated glass has lower emissivity than paints, it absorbs less solar radiated power. Therefore, $CaCO_3$ can exhibit more cooling than that shown by paint under incident solar radiation.

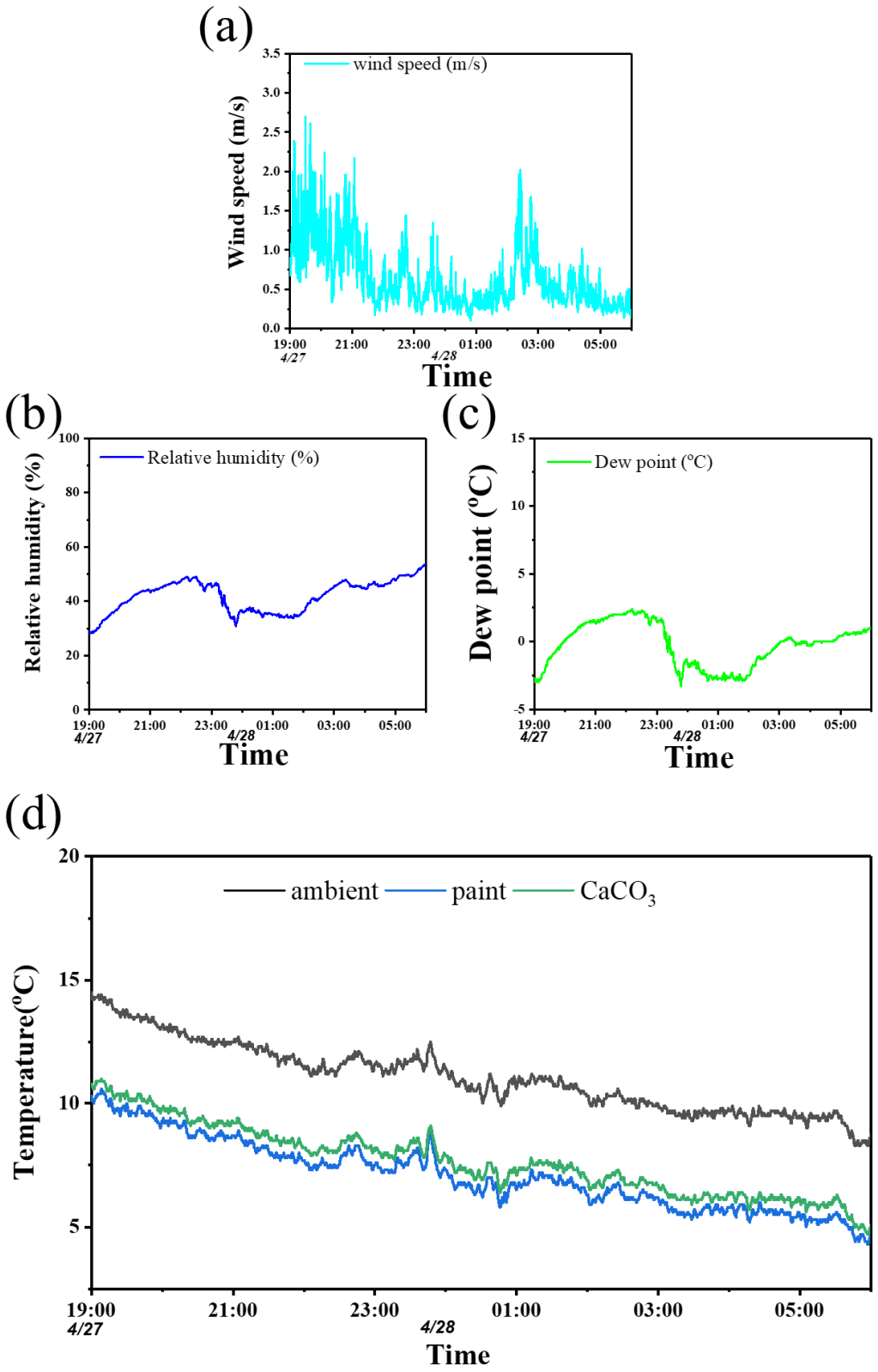

Figure. 4. Environmental conditions (a) wind speed, (b) Relative humidity, (c) dew point. (d) Radiative cooling performance of $CaCO_3$ and white paint in terms of temperature in nighttime.

Similarly, the wind speed, relative humidity, and dew point at nighttime (19:00 to 5:00) are presented in Figure 4(a), (b), and (c), respectively. Figure 4(d) depicts the radiative coolers and the ambient temperature. Because it is nighttime, the solar irradiance is 0, and the heating caused by solar irradiance does not affect the performance of radiative cooling: only emission does. Therefore, paint, which has a higher emissivity than that of $CaCO_3$, exhibits slightly better cooling performance—$CaCO_3$ cooled by 3.38 ℃ and paint cooled by 3.93 ℃. The average cooling temperatures of the $CaCO_3$- and paint-coated glasses during daytime and nighttime are listed in Table 2. The values indicate that both the samples can exhibit cooling to below the ambient temperature during both daytime and nighttime.

Table 2. Average cooling temperature in daytime and nighttime.

Sample	Average cooling temperature (10:00-15:00)	Average cooling temperature (19:00-06:00)
paint	-0.93 ℃	-3.93 ℃
$CaCO_3$	-6.52 ℃	-3.38 ℃

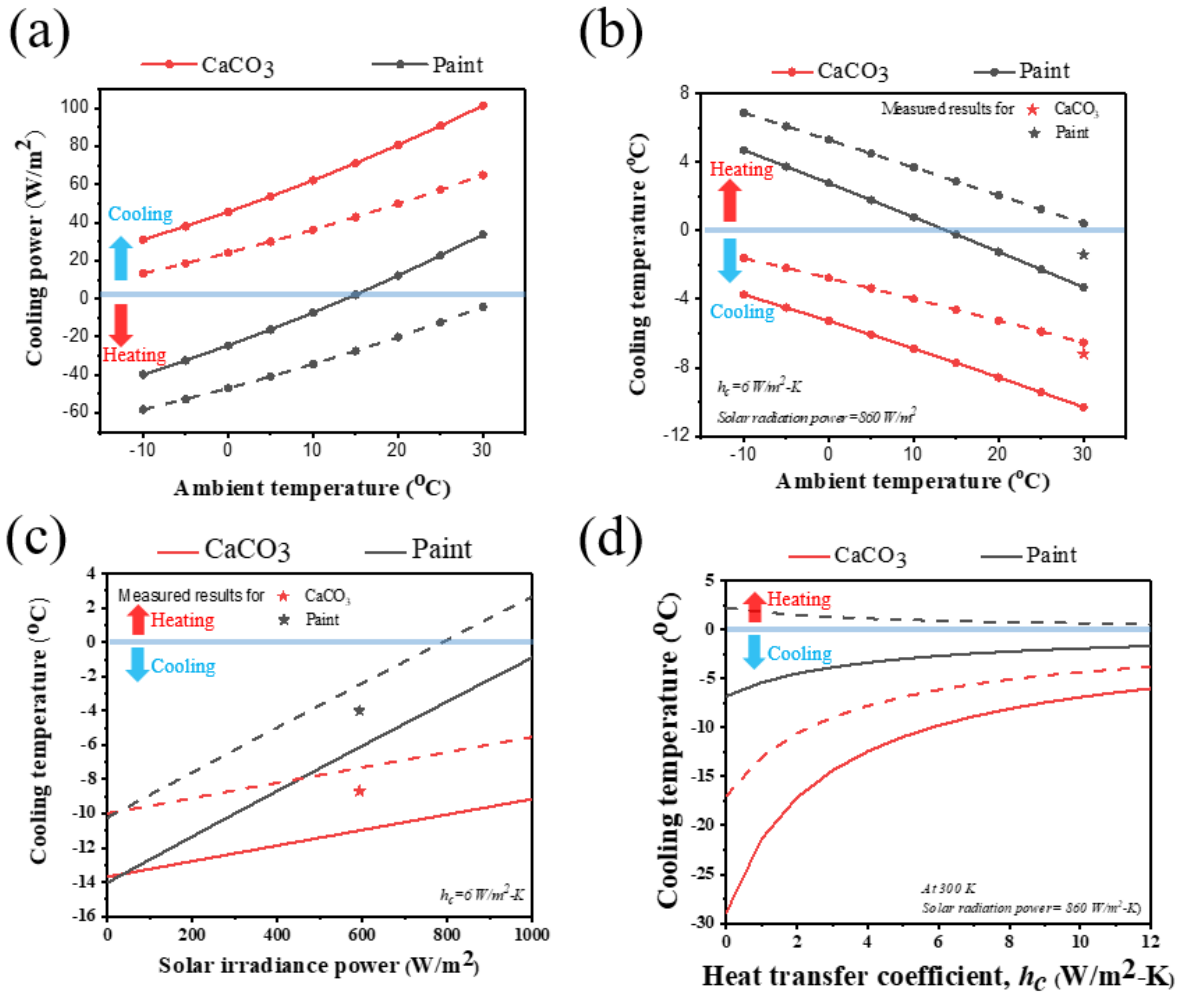

231

232 **Figure. 5**. (a) Calculated cooling power of $CaCO_3$ and (b) cooling temperature in accordance with ambient
233 temperature under the condition of h_c = 6 W/m^2-K using ideal (solid line) and mid-latitude winter (dotted line)
234 atmospheric transmittance and measured cooling temperatures are represented with stars (red for $CaCO_3$/glass,
235 gray for paint/glass). (c) Calculated temperatures of $CaCO_3$- and paint-coated glass in accordance with the solar
236 irradiance power under the condition of h_c = 6 W/m^2-K and measured cooling temperatures are marked with stars
237 (red for $CaCO_3$, gray for paint). (d) Calculated temperatures of $CaCO_3$- and paint-coated glass in accordance with
238 convection coefficient h_c at 300 K using AM1.5 solar irradiance spectrum using ideal (solid line) and mid-latitude
239 (dotted line) atmospheric transmittance.

240 Figure 5(a) and (b) depict the calculated cooling power and temperature in accordance with the
241 ambient temperature at a steady state. The solar irradiance density and atmospheric
242 transmittance used in the calculation are depicted in Figure S3. The heat transfer coefficient is
243 assumed to be 6 W/m^2-K in consideration of the wind speed (about 1-1.5 m/s) in Figure 3(b)
244 under condition of the wind cover according to the literature equation[40]. Under ideal
245 transmittance, $CaCO_3$ and the paint can cool by approximately 10 °C and 4 °C, respectively,

246 and they have cooling powers of 93.1 and 38.6 W/m^2, respectively, at 300 K. However, the
247 measured results indicate a lower cooling performance when compared with the calculated
248 results. This is attributed to the effect of the weather at the time of the measurement and the
249 climatic characteristics of the mid-latitude region as well as the LDPE film, which make the
250 atmospheric transmittance lower than the ideal one. Based on the mid-latitude atmospheric
251 transmittance obtained by calculation using MODTRAN 6, the results indicate that $CaCO_3$ and
252 the paint can cool by approximately 6 and 0.6 ℃, respectively, and that they have cooling
253 powers of 60 and 6 W/m^2, respectively. Compared with the actual measurement, these results
254 indicate a more similar cooling performance when using the mid-latitude atmospheric
255 transmittance, in contrast with the results obtained assuming ideal transmittance. Owing to the
256 difference between the assumed (888 W/m^2) and actual solar irradiances (< 888 W/m^2), the
257 measured cooling temperature is slightly higher than the calculated data. According to the
258 Stefan–Boltzmann law, the total energy radiated from a blackbody is proportional to the fourth
259 power of temperature. As depicted in Figure 3 and Figure 4, even though there is no sunlight
260 at night, the cooling temperature is less than that during the daytime because, based on this law,
261 the cooler radiates less energy. Figure 5(a) and (b) also indicate the same tendency, in
262 accordance with this law. Figure 5(c) depicts the cooling temperature with respect to the solar
263 irradiance power using ideal and mid-latitude atmospheric transmittance with a heat transfer
264 coefficient of 6 W/m^2-K. When the solar irradiance power is zero, $CaCO_3$ can cool to
265 approximately 14 °C below ambient temperature under ideal atmospheric transmittance and to
266 10 °C below ambient temperature under mid-latitude transmittance, and the paint can cool to
267 almost the same extent as $CaCO_3$ at 300 K. Because there is no sunlight, only emissivity in the
268 atmospheric window affects the radiative cooling performance. Therefore, compared with
269 $CaCO_3$, the paint, which has higher average emissivity of 3%p, can cool slightly more.

However, as the solar irradiance power increases, the temperatures of $CaCO_3$ and the paint differ gradually. When solar irradiance power reaches 1000 W/m^2, $CaCO_3$ can cool by approximately 9 °C under ideal transmittance and by 5.3 ℃ under mid-latitude transmittance; further, the paint can cool by 2.6 ℃ under ideal transmittance, and its temperature increases to 1 ℃ under mid-latitude transmittance. Under strong solar irradiance, not only the emissivity in the transmittance window but also the ability to reflect sunlight is significant. Therefore, It is demonstrated that $CaCO_3$ has much better cooling performance than paint as the solar irradiance power increases. There are slight differences between the calculated and measured data because the actual and calculated values of the atmospheric transmittance and heat transfer coefficient differ. Figure 5(d) depicts the cooling temperature of the $CaCO_3$- and paint-coated glasses in accordance with the heat transfer coefficient, h_c, under the solar irradiance power of 888 W/m^2. When h_c = 0, which is similar to the case of vacuum, $CaCO_3$ can cool by 28 ℃ under ideal transmittance and by 16 ℃ under mid-latitude transmittance, and the paint can cool by 10 ℃ under ideal transmittance and by 0.7 ℃ under mid-latitude transmittance. As the value of h_c increases, parasitic heat exchange occurs in the ambient environment and reduces the cooling performance. Even when h_c = 12 W/m^2-K, at which heat exchange occurs actively via conduction and convection, $CaCO_3$ can cool by 6 ℃ under ideal transmittance and by 4 ℃ under reduced transmittance. In contrast, the paint cooled by 2.4 ℃ under ideal transmittance, and even at the reduced transmittance in h_c value is 0, it cooled by less than 1 ℃ because it exhibits substantial absorption of solar irradiance. Thus, both actual measurements and calculations show that $CaCO_3$ demonstrates better cooling performance than the paint.

5. Conclusions

In this work, we demonstrated the radiative cooling performance of $CaCO_3$ microparticles both by calculation and experiment. As the proposed device has a powder-based layer, the scattering effect maximizes the reflectance for solar irradiance wavelengths; further, owing to the intrinsic optical properties of $CaCO_3$, this device can emit energy in the form of infrared (8−13 μm) rays. Notably, this device absorbs only 4% of the radiated solar power and exhibits an average emissivity of approximately 90% in the atmospheric window. Through actual measurements of temperature variations, it is demonstrated that the $CaCO_3$ radiative cooler can cool by 6.5 ℃ during the daytime and by 3.4 ℃ during nighttime. Further, according to calculations, it can cool by more than 10 ℃ during daytime. Furthermore, this structure, $CaCO_3$ composite single layer, does not contain any metal layer as reflector, which enhances productivity, price competitiveness and practicality. These results demonstrate that the proposed $CaCO_3$ can be employed as a radiative cooler itself. Owing to the property of $CaCO_3$, it can be radiative cooler as tile of paint forms and can be applied to building, car, cool bag or other any fields that need being cooled.

Associated content

Supporting Information

XRD results for $CaCO_3$ powders; Optical properties of $CaCO_3$-based radiative cooler in accordance with thickness; Solar power density and atmospheric transmittance window

Corresponding Authors

E-mail: nanoimprint@naver.com.

CRediT authorship contribution statement

Hangyu Lim: Conceptualization, Methodology, Writing-Original draft, Visulization, Formal analysis, Investigation. **Dongwoo Chae**: Conceptualization, Software, Validation. **Soomin Son**: Resources, Methodology. **Sucheol Ju**: Data Curation. **Jisung Ha**: Investigation. **Heon Lee**: Supervision

Acknowledgements

This research was supported by Creative Materials Discovery Program through the National Research Foundation of Korea(NRF) funded by Ministry of Science and ICT (NRF-2018M3D1A1058972). This work was supported by the National Research Foundation of Korea(NRF) grant funded by the Korea government(MSIT) (No. 2020R1A2C3006382). This research was supported by the International Research & Development Program of the National Research Foundation of Korea (NRF) funded by the Ministry of Science and ICT (Grant number: 2019K1A47A02113032)

References

1. EPA. Phaseout of Ozone-Depleting Substances. *US Environ. Prod. Agency* (2016).

2. Raman, A. P., Anoma, M. A., Zhu, L., Rephaeli, E. & Fan, S. Passive radiative cooling below ambient air temperature under direct sunlight. *Nature* 515, 540–544 (2014).

3. Zhao, B., Hu, M., Ao, X., Chen, N. & Pei, G. Radiative cooling: A review of fundamentals, materials, applications, and prospects. *Applied Energy* vol. 236 489–513 (2019).

4. Mandal, J. *et al*. Hierarchically porous polymer coatings for highly efficient passive daytime radiative cooling. *Science* (80-.). 362, 315–319 (2018).

5. Chae, D., Son, S., Liu, Y., Lim, H. & Lee, H. High-Performance Daytime Radiative Cooler and Near-Ideal Selective Emitter Enabled by Transparent Sapphire Substrate. *Adv. Sci*. 7, 2001577 (2020).

6. Rephaeli, E., Raman, A. & Fan, S. Ultrabroadband photonic structures to achieve high-performance daytime radiative cooling. *Nano Lett*. 13, 1457–1461 (2013).

7. Chae, D. *et al*. Spectrally Selective Inorganic-Based Multilayer Emitter for Daytime Radiative Cooling. *ACS Appl. Mater. Interfaces* 12, 8073–8081 (2020).

8. Zhai, Y. *et al*. Scalable-manufactured randomized glass-polymer hybrid metamaterial for daytime radiative cooling. *Science* (80-.). 355, 1062–1066 (2017).

9. Zhou, L. *et al*. A polydimethylsiloxane-coated metal structure for all-day radiative cooling. *Nat. Sustain*. 2, 718–724 (2019).

10. Suichi, T., Ishikawa, A., Tanaka, T., Hayashi, Y. & Tsuruta, K. Whitish daytime radiative cooling using diffuse reflection of non-resonant silica nanoshells. *Sci. Rep*. 10, 1–6 (2020).

11. Lee, D. *et al*. Sub-ambient daytime radiative cooling by silica-coated porous anodic aluminum oxide. *Nano Energy* 79, 105426 (2021).

12. Lee, G. J., Kim, D. H., Heo, S. Y. & Song, Y. M. Spectrally and Spatially Selective Emitters Using Polymer Hybrid Spoof Plasmonics. *ACS Appl. Mater. Interfaces* 12, 53206–53214 (2020).

13. Didari, A. & Mengüç, M. P. A biomimicry design for nanoscale radiative cooling applications inspired by Morpho didius butterfly. *Sci. Rep*. 8, 16891 (2018).

14. Zhu, L., Raman, A., Wang, K. X., Anoma, M. A. & Shanhui Fan, A. Radiative cooling of solar cells. (2014) doi:10.1364/OPTICA.1.000032.

15. Bhatia, B. *et al*. Passive directional sub-ambient daytime radiative cooling. *Nat. Commun*. 9, 1–8 (2018).

16. Son, S. *et al*. Colored emitters with silica-embedded perovskite nanocrystals for efficient daytime radiative cooling. *Nano Energy* 105461 (2020) doi:10.1016/j.nanoen.2020.105461.

17. Lv, S. *et al*. A novel strategy of enhancing sky radiative cooling by solar photovoltaic-thermoelectric cooler. *Energy* 219, 119625 (2021).

18. Rajkhowa, R. Light Pollution and Impact of Light Pollution. *International Journal of Science and Research www.ijsr.net.*

19. Xiang, B. *et al*. 3D porous polymer film with designed pore architecture and auto-deposited SiO2 for highly efficient passive radiative cooling. *Nano Energy* 81, 105600 (2021).

20. Chen, Y. *et al*. Cellulose-Based Hybrid Structural Material for Radiative Cooling. *Nano Lett*. 21, 404 (2021).

21. Bijarniya, J. P., Sarkar, J. & Maiti, P. Performance simulation of polymer-based nanoparticle and void dispersed photonic structures for radiative cooling. *Sci. Rep*. 11, 893 (2021).

22. Son, S., Liu, Y., Chae, D. & Lee, H. Cross-Linked Porous Polymeric Coating without a Metal-Reflective Layer for Sub-Ambient Radiative Cooling. *ACS Appl. Mater. Interfaces* 12, 57839 (2021).

23. Sun, S., Li, C., Zhang, L., Du, H. & Burnell-Gray, J. Interfacial structures and mechanical properties of PVC composites reinforced by CaCO3 with different particle sizes and surface treatments. *Polym. Int*. 55, 158–164 (2006).

24. Chen, C.-H., Teng, C.-C., Su, S.-F., Wu, W.-C. & Yang, C.-H. Effects of microscale calcium carbonate and nanoscale calcium carbonate on the fusion, thermal, and mechanical characterizations of rigid poly(vinyl chloride)/calcium carbonate composites. *J. Polym. Sci. Part B Polym. Phys*. 44, 451–460 (2006).

25. Liu, P., Zhao, M. & Guo, J. Thermal Stabilities of Poly(Vinyl Chloride)/Calcium Carbonate (PVC/CaCO 3) Composites. *J. Macromol. Sci. Part B* 45, 1135–1140 (2006).

26. Abdolmohammadi, S. *et al*. Enhancement of Mechanical and Thermal Properties of Polycaprolactone/Chitosan Blend by Calcium Carbonate Nanoparticles. *Int. J. Mol. Sci*. 13, 4508–4522 (2012).

27. Mizuno, M., Fukunaga, K., Saito, S. & Hosako, I. Analysis of calcium carbonate for differentiating between pigments using terahertz spectroscopy. *J. Eur. Opt. Soc. Rapid Publ*. 4, 9044 (2009).

28. Sun, S., Ding, H. & Hou, X. Preparation of CaCO3-TiO2 Composite Particles and Their Pigment Properties. Materials (Basel). 11, 1131 (2018).

29. Deng, C.-M., Chen, M., Ao, N.-J., Yan, D. & Zheng, Z.-Q. CaCO3/natural rubber latex nanometer composite and its properties. *J. Appl. Polym. Sci*. 101, 3442–3447 (2006).

30. Ahmad, W., Singh, B., Dalal, R. C. & Dijkstra, F. A. Carbon dynamics from carbonate dissolution in Australian agricultural soils. *Soil Res*. 53, 144 (2015).

31. Rocha, D. B., Souza de Carvalho, J., de Oliveira, S. A. & dos Santos Rosa, D. A new approach for flexible PBAT/PLA/CaCO 3 films into agriculture. *J. Appl. Polym. Sci*. 135, 46660 (2018).

32. Trushina, D. B., Bukreeva, T. V., Kovalchuk, M. V. & Antipina, M. N. CaCO3 vaterite microparticles for biomedical and personal care applications. *Mater. Sci. Eng*. C 45, 644–658 (2014).

33. Fujiwara, M. *et al*. Encapsulation of proteins into CaCO3 by phase transition from vaterite to calcite. Cryst. *Growth Des*. 10, 4030–4037 (2010).

34. Suppes, G. J. et al. Calcium carbonate catalyzed alcoholysis of fats and oils. *JAOCS, J. Am. Oil Chem. Soc*. 78, 139–145 (2001).

35. Chunxiang, Q., Jianyun, W., Ruixing, W. & Liang, C. Corrosion protection of cement-based building materials by surface deposition of CaCO3 by Bacillus pasteurii. *Mater. Sci. Eng*. C 29, 1273–1280 (2009).

36. Galván-Ruiz, M., Hernández, J., Baños, L., Noriega-Montes, J. & Rodríguez-García, M. E. Characterization of Calcium Carbonate, Calcium Oxide, and Calcium Hydroxide as Starting Point to the Improvement of Lime for Their Use in Construction. *J. Mater. Civ. Eng*. 21, 694–698 (2009).

37. Hossain, M. M. & Gu, M. Radiative cooling: Principles, progress, and potentials. *Advanced Science* vol. 3 (2016).

38. Aili, A. *et al*. A kW-scale, 24-hour continuously operational, radiative sky cooling system: Experimental demonstration and predictive modeling. *Energy Convers. Manag*. 186, 586–596 (2019).

39. Zhao, D. *et al*. Subambient Cooling of Water: Toward Real-World Applications of Daytime Radiative Cooling. *Joule* 3, 111–123 (2019).

40. Liu, J. *et al*. Sub-ambient radiative cooling with wind cover. *Renew. Sustain. Energy Rev*. 130, 109935 (2020).

41. Liu, J. *et al*. Performance evaluation of various strategies to improve sub-ambient radiative sky cooling. *Renew. Energy* 169, 1305–1316 (2021).

441

Figures

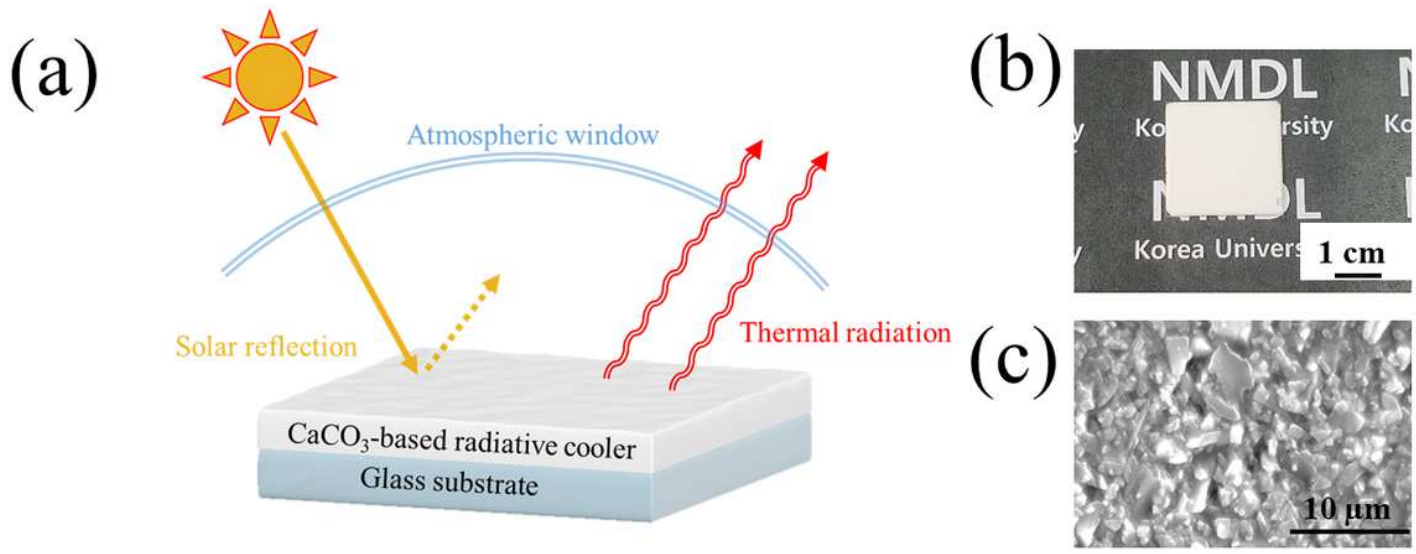

Figure 1

(a) Schematic of radiative cooling principle and radiative cooler structure. (b) Photo image and (c) SEM top view of radiative cooler, CaCO3-coated glass.

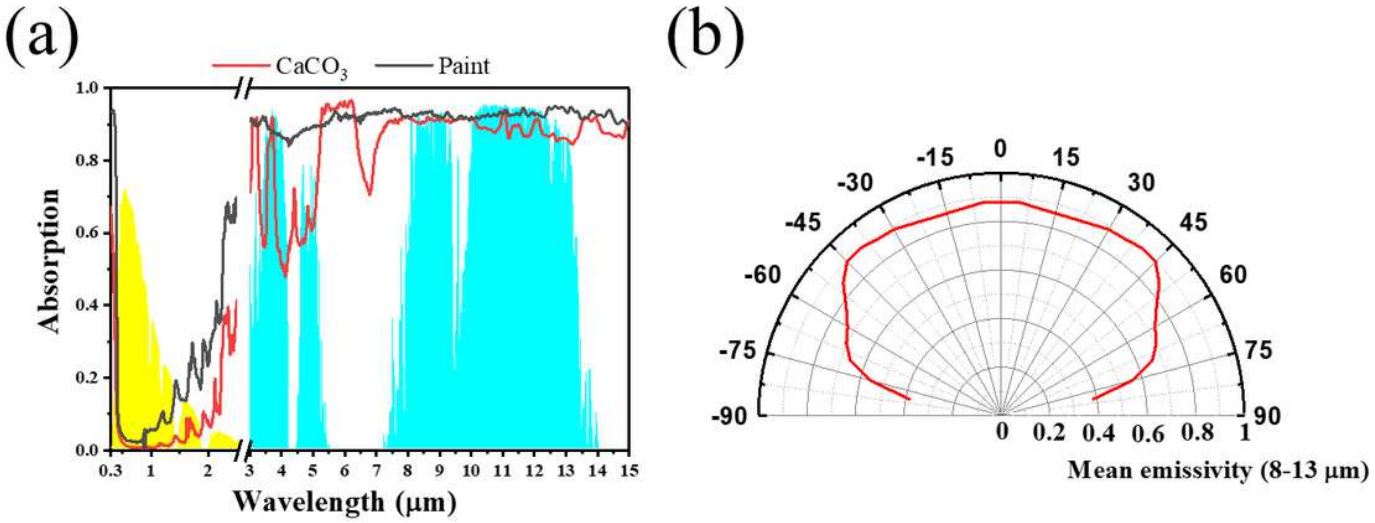

Figure 2

(a) Spectral absorptivity and emissivity of CaCO3- and commercial white-paint-coated glass. (b) Average emissivity of CaCO3-coated glass in the atmospheric window (8–13 μm) with respect to angle θ.

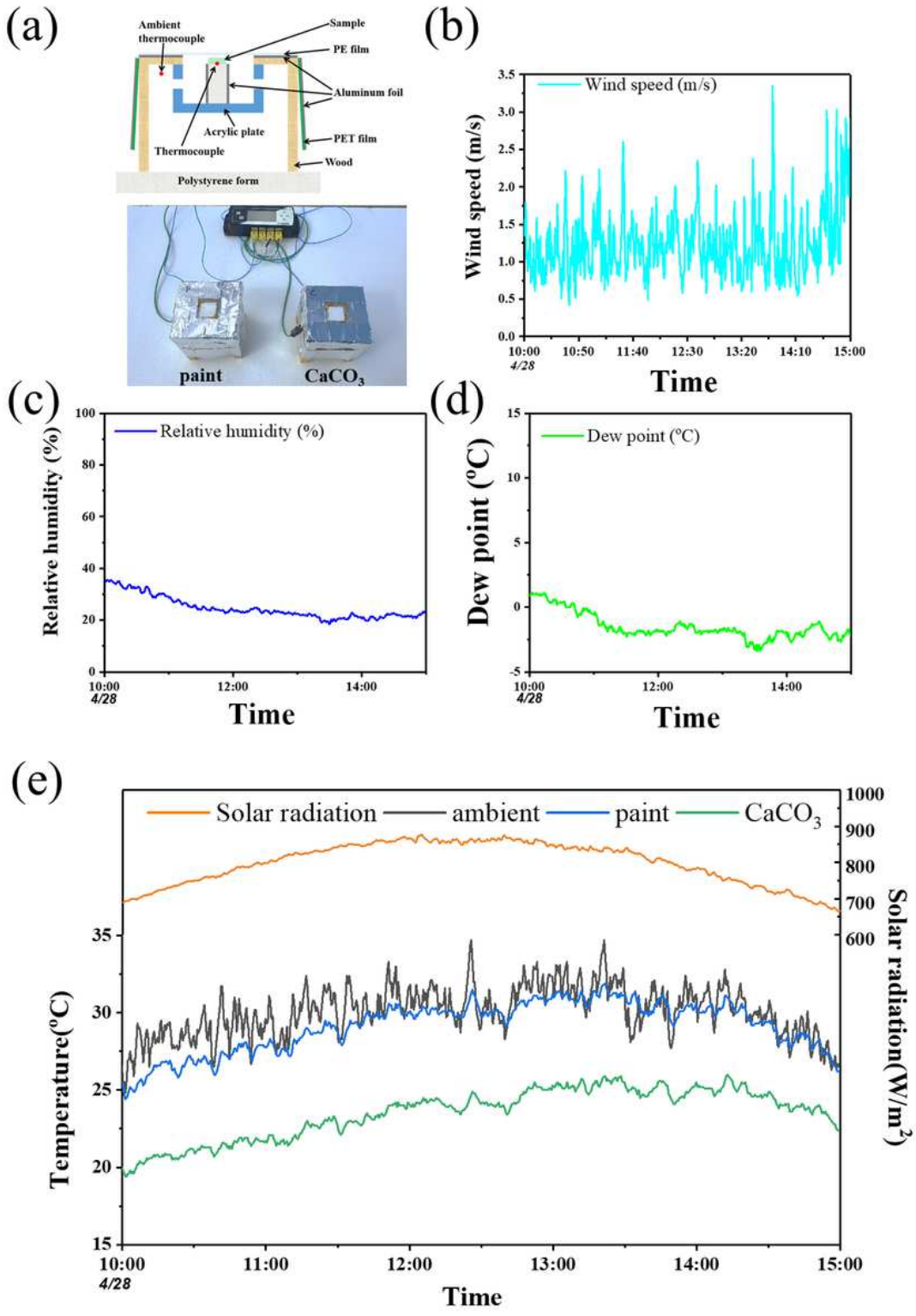

Figure 3

(a) Schematic diagram and photo image of outdoor measurement system for radiative cooling. Environmental conditions (b) wind speed, (c) Relative humidity, (d) dew point. (e) Radiative cooling performance of CaCO3 and white paint in terms of temperature in daytime.

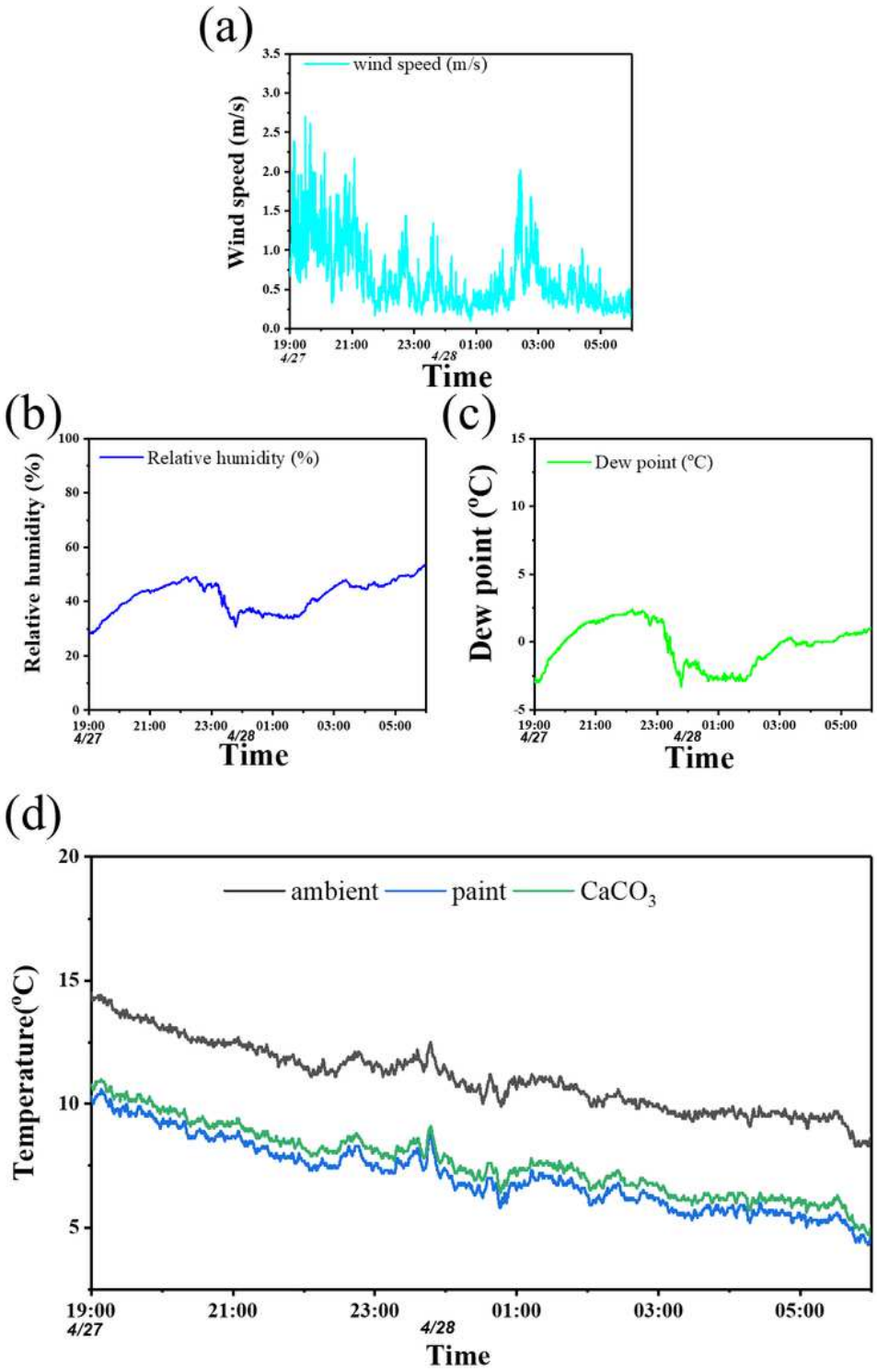

Figure 4

Environmental conditions (a) wind speed, (b) Relative humidity, (c) dew point. (d) Radiative cooling performance of CaCO3 and white paint in terms of temperature in nighttime.

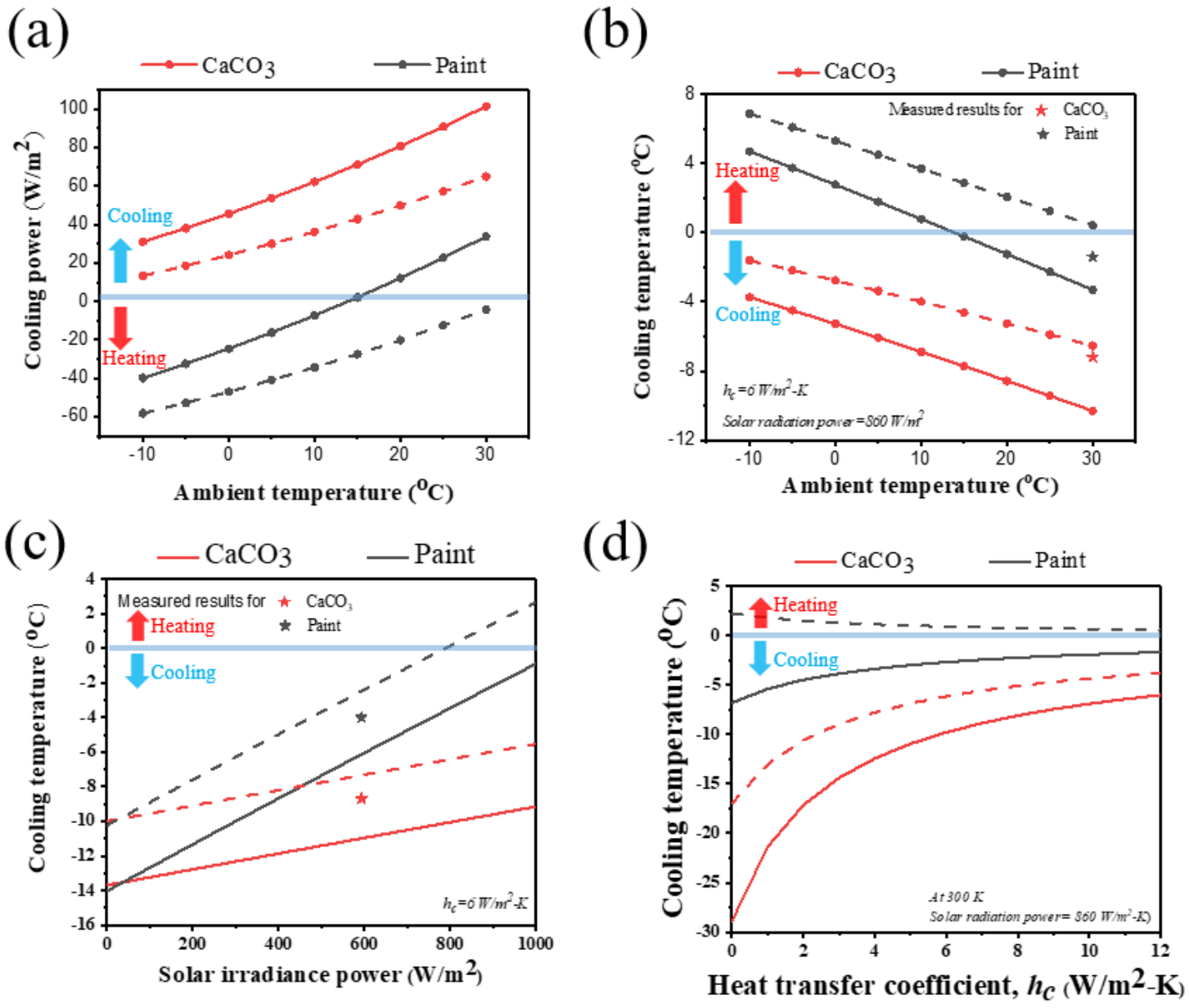

Figure 5

(a) Calculated cooling power of CaCO3 and (b) cooling temperature in accordance with ambient temperature under the condition of hc = 6 W/m2-K using ideal (solid line) and mid-latitude winter (dotted line) atmospheric transmittance and measured cooling temperatures are represented with stars (red for CaCO3/glass, gray for paint/glass). (c) Calculated temperatures of CaCO3- and paint-coated glass in accordance with the solar irradiance power under the condition of hc = 6 W/m2-K and measured cooling temperatures are marked with stars (red for CaCO3, gray for paint). (d) Calculated temperatures of CaCO3- and paint-coated glass in accordance with convection coefficient hc at 300 K using AM1.5 solar irradiance spectrum using ideal (solid line) and mid-latitude (dotted line) atmospheric transmittance.

Supplementary Files

This is a list of supplementary files associated with this preprint. Click to download.

- supporting.docx
- Graphicalabstract.png